JACS
JOURNAL OF THE AMERICAN CHEMICAL SOCIETY

ARTICLE

pubs.acs.org/JACS

Molecular Dynamics of Proteorhodopsin in Lipid Bilayers by Solid-State NMR

Jun Yang,*[,†,‡] Lubica Aslimovska,[†] and Clemens Glaubitz*[,†]

[†]Institute for Biophysical Chemistry & Centre for Biomolecular Magnetic Resonance, Goethe University Frankfurt/M., Max-von-Laue Strasse 9, 60438 Frankfurt/M., Germany

[‡]State Key Laboratory of Magnetic Resonance and Atomic and Molecular Physics, Wuhan Center for Magnetic Resonance, Wuhan Institute of Physics and Mathematics, The Chinese Academy of Sciences, Wuhan 430071, China

Supporting Information

ABSTRACT: Environmental factors such as temperature, hydration, and lipid bilayer properties are tightly coupled to the dynamics of membrane proteins. So far, site-resolved data visualizing the protein's response to alterations in these factors are rare, and conclusions had to be drawn from dynamic data averaged over the whole protein structure. In the current study, high-resolution solid-state NMR at high magnetic field was used to investigate their effects on the molecular dynamics of green proteorhodopsin, a bacterial light-driven proton pump. Through-space and through-bond correlation experiments were employed to identify and characterize highly mobile and motionally restricted regions of proteorhodopsin. Our data show that hydration water plays an essential role for enhancing molecular dynamics of residues in tails and interhelical loops, while it is found less important for residues in transmembrane domains or rigid, structured loop segments. In contrast, switching the lipids from the gel to their liquid crystalline phase enhances molecular fluctuations mainly in transmembrane helices on a time scale of 10^{-6} s, but has little effect on loop and tail residues. Increased mobility is especially observed in helices C, F, and G, but also in the EF loop. Fluctuations in those regions are relevant to structural dynamics during the photocycle of proteorhodopsin. Our data are important for the functional understanding of proteorhodopsin, but also offer an important contribution to the general understanding of site-resolved effects of water and lipid bilayers onto the dynamic properties of membrane proteins.

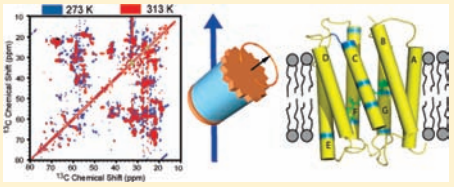

INTRODUCTION

Motions at different amplitudes and time scales are crucial for the function of membrane proteins, which are embedded in lipid bilayers and exposed to water at the water−membrane interface. Environmental factors such as temperature, hydration, and lipids have a profound influence on the structure, function and dynamics of membrane proteins. It is therefore essential to consider them not as isolated polypeptide entities but as lipid−protein−water complexes,[1−3] which has been in the focus of a number of studies. For example, neutron scattering data on bacteriorhodopsin (BR) in purple membrane did show that picosecond fluctuations required for conformational changes during the photocycle are tightly coupled to the amount of water interacting with lipid and protein.[4] Furthermore, delipidation causes significant inhibition of protein function and dynamics.[5] Solid-state NMR has shown that low frequency motions at approximately 10^{-5} s within membrane proteins are strongly affected by the degree of hydration.[6] It has been even shown for rhodopsin that the degree of internal hydration varies with the functional state of the protein.[7] The influence of these factors on membrane protein dynamics is also supported by molecular dynamics simulations.[8,9] These studies offered a valuable general view of the complex interplay between protein dynamics, hydration, and lipid environment, but there is a lack of site-resolved data. Usually, α-helical membrane proteins consist of transmembrane helical bundles connected by intra- and extracellular loops. This architecture may result in very different molecular dynamic time scales and amplitudes within the protein.[10] To what extent these different motional regimes are influenced by hydration and lipid environment has not been addressed so far. Here, we have investigated the influence of water, lipid bilayer properties, and temperature on the molecular dynamics of the 7-helical transmembrane proton pump proteorhodopsin by taking advantage of multidimensional through-bond and through-space magic angle sample spinning (MAS) NMR correlation experiments based on J- and dipolar couplings at very high field (850 MHz ^{1}H Larmor frequency).

Proteorhodopsins (PR) are retinal proteins, found in high abundance in bacteria in the photic zone of the oceans.[11,12] The green absorbing form (27 kDa, $\lambda_{max} \approx 520$ nm) was found to function as a light-driven proton pump.[13,14] Similar to BR, green PR contains a primary proton acceptor (D97), a proton donor (E108), a Schiff base (K231), and counterions of the Schiff base (R94, D227).[14] Different from BR is its lack of a proton release group, a histidine close to the active site (H75), and an unusually high pK_a of the primary proton acceptor.[14] A complete 3D structure has not been determined yet. Atomic force microscopy (AFM), electron microscopy (EM), as well as mass spectrometry

Received: October 30, 2010
Published: March 14, 2011

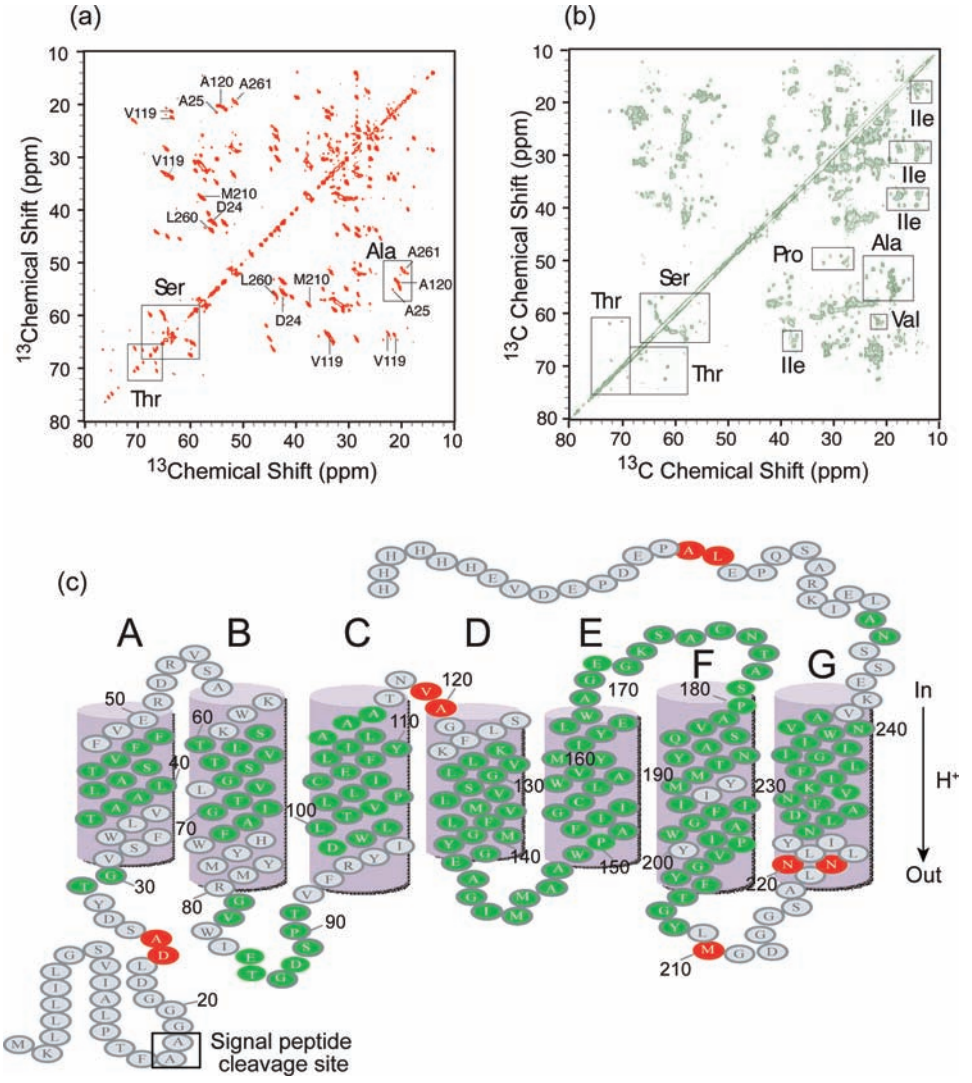

Figure 1. Comparison of the aliphatic regions of (a) CC-INEPT-TOBSY and (b) CC-DARR experiments of U-[^{13}C,^{15}N]-PR. Only a small number of residues contribute to INEPT-TOBSY spectrum. Both spectra were acquired at 273 K (see text for further details). (c) Topology plot of PR with J-residues (red), D-residues (green), and unassigned residues (gray). The topology is based on prediction and solid-state NMR constraints.[19]

have shown that PR assembles into pentameric or hexameric complexes.[15−17] Topology analysis, homology modeling, and most recently solid-state NMR studies have confirmed that PR follows the typical 7 transmembrane helix topology (Figure 1c).[14,18−20] Solid-state NMR has been also used to probe the photoactive center of PR.[21,22] A first global view at the structural dynamics of PR during the photo cycle has been obtained by wide-angle X-ray scattering (WAXS).[23]

Solid-state NMR is a powerful tool to probe protein dynamics within a lipid environment.[24−27] In contrast to liquid-state NMR, motional correlation times can be measured from microseconds to milliseconds because spin relaxation and NMR line shapes are not dominated by fast isotropic molecular tumbling. The application of high fields in combination with homo- and heteronuclear MAS NMR correlation experiments allows resonance assignment and opens the door for obtaining site-specific dynamic data.[28−32] In the work presented here, the molecular dynamics of PR within lipid bilayers has been studied by ^{13}C-MAS NMR, which allows probing two major motional regimes covering different amplitudes and time scales:[10,32] (a) Molecular segments engaged in fast, large amplitude fluctuations on time scales of $<10^{-5}$ s lead to solution-state-like spectra due to efficient molecular averaging of anisotropic interactions. This enables detection of mobile molecular segments by utilizing experiments based on magnetization transfer through J-couplings. We will refer in the following to residues visible in such experiment as "J-residues". (b) Molecular segments with smaller amplitude motions, which are not sufficient to fully average anisotropic interactions (such as HH, HC, or HN dipole couplings), can be observed in experiments in which initial magnetization is achieved through dipolar couplings by cross-polarization. We will refer in the following to residues in this category as "D-residues".

We have investigated the molecular dynamics of PR in its ground state through the response of both J- and D-residues with respect to water interaction, temperature changes, and alterations in membrane elasticity. Characterizing ground-state dynamics of PR reveals regions with enhanced thermal fluctuations, which are of functional importance.

RESULTS

a. Identification of J-Residues in PR. To identify which residues belong to the "J" or "D" categories as defined above, we

dx.doi.org/10.1021/ja109766n |J. Am. Chem. Soc. 2011, 133, 4874–4881

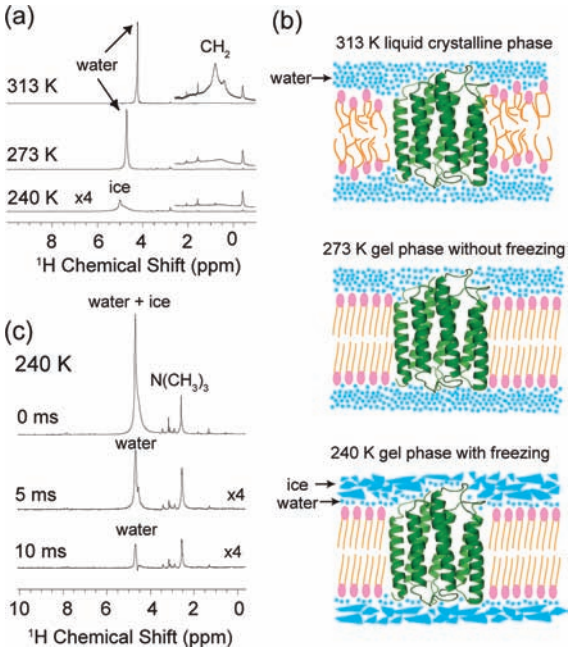

Figure 2. ^{1}H-MAS spectra of U-[^{13}C,^{15}N]$_{\backslash WHYFI}$-PR in DMPC/DMPA lipid bilayers allow monitoring of temperature-induced water and lipid phase transitions (a). Illustration of the three different temperature regimes (b) monitored by ^{1}H MAS NMR. ^{1}H spin echo spectra recorded at 240 K with 0, 5, and 10 ms ^{1}H-T_2' echo delay reveals that water within the first hydration layer is still highly mobile. Only narrow water signals are selected, while broad resonances from "solid-like" frozen ice crystals are suppressed (c).

have employed two different magnetization transfer schemes. Mobile "J-residues" have been selected by creating ^{13}C magnetization using a refocused INEPT transfer step, which transfers magnetization from mobile protons to carbons via J-couplings. ^{13}C−^{13}C correlation between these carbons has been established through carbon−carbon J-couplings using total through-bond-correlation spectroscopy (CC-INEPT-TOBSY).[31] On the other hand, "D-residues" are selected by creating initial ^{13}C magnetization through cross-polarization (CP), which is based on ^{1}H−^{13}C dipolar coupling. ^{13}C−^{13}C through-space correlations are observed through dipolar-assisted rotational resonance (CC-DARR).[33] The CC-INEPT-TOBSY (Figure 1a) shows much fewer correlations than the CC-DARR spectrum (Figure 1b). This means that only a small number of residues are involved in fast, large amplitude motions. The line width of isolated cross peaks in Figure 1a is between 0.3 and 0.5 ppm and in Figure 1b is between 0.5 and 0.7 ppm.

For sequential assignment of J-residues, we have carried out INEPT-based 2D-(H)N(CO)CA, (H)NCA, (H)NCO, and H-(C)C heteronuclear correlation (HETCOR) experiments (partially shown in Figure S2). Six residues could be assigned unambiguously (D24, A25, V119, A120, L260, A261), and we were able to identify 11 more amino acids by their types (1 × T, 3 × S, 3 × N, 1 × L, 1 × D, 1 × Y, 1 × A). Residues M210, N219, and N220 have been assigned tentatively on the basis of amino acid type and chemical shift-based secondary structure prediction (Table S1).[34] Overall, the number of J-residues is relatively small. Their locations are highlighted in the topology plot in Figure 1c (red). For completeness, 153 D-residues as assigned previously[18,19] are labeled in green.

b. Effect of Hydration and Lipids on the Dynamics of J- and D-Residues. Experiments described so far were carried

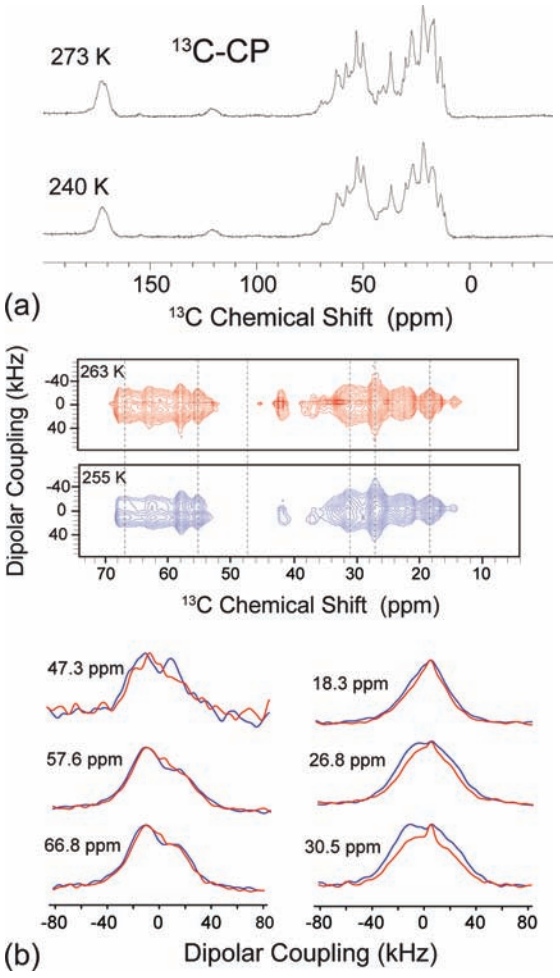

Figure 3. (a) ^{13}C-CP spectra of U-[^{13}C,^{15}N]-PR at 273 and 240 K. (b) WISE spectra above (263 K) and below (255 K) the freezing point of the water. The freezing of water at 255 K was monitored by ^{1}H MAS spectra.

out on PR reconstituted in DMPC/DMPA lipid bilayers at 273 K. To probe the effect of temperature onto the dynamics of PR, we have chosen three different regimes, in which (i) the protein is dehydrated by freezing of bulk water and lipids are in their gel phase (T = 240 K); (ii) lipids are in their gel phase but water is not frozen (T = 273 K); and (iii) lipids are found in their liquid crystalline phase (T = 313 K). These three situations have been controlled by monitoring the ^{1}H chemical shift and line width of water and lipid CH_2 resonances (Figure 2a). The lipid CH_2 peak is very broad in the gel phase and becomes narrow in the fluid phase, while the water resonance becomes broad if ice is formed. All three regimes are illustrated in Figure 2b. At 240 K, there is still a layer of nonfrozen hydration water, as shown by ^{1}H spin echo experiments (Figure 2c).

The overall signal intensity of ^{13}C-CP spectra of U-[^{13}C,^{15}N]-PR is almost comparable in both gel phase spectra at 240 and 273 K, independent of whether water is frozen or not (Figure 3a). However, considerable line broadening is observed in CC-DARR spectra at 240 K (not shown here), which is consistent with previous studies of BR and peptides in lipid bilayers and arises from a distribution of local conformations after freezing of bulk water.[35,36] To further probe dynamics on the submicrosecond time scale below (255 K) and above (263 K) the freezing point of water, we have recorded two-dimensional wide line separation

dx.doi.org/10.1021/ja109766n |J. Am. Chem. Soc. 2011, 133, 4874–4881

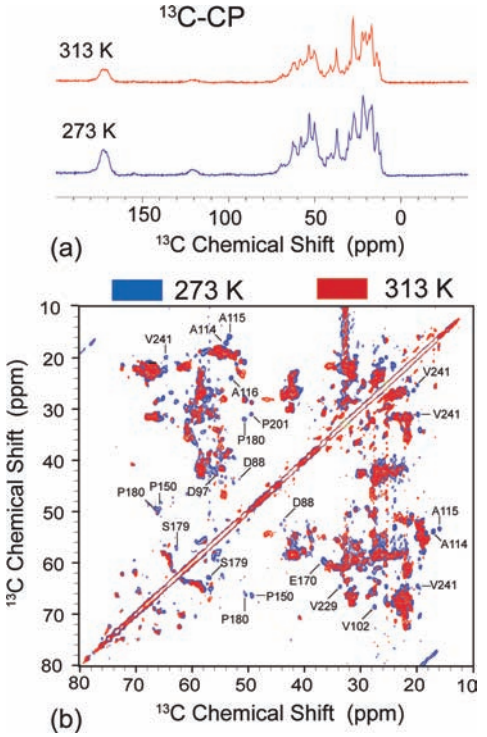

Figure 4. ^{13}C-CP spectra (a) and the aliphatic regions of CC-DARR spectra (b) of U-[^{13}C,^{15}N]$_{\backslash WHYFI}$-PR at 273 (blue, gel phase) and 313 K (red, liquid crystal phase). Peaks disappearing in the liquid crystal phase are labeled (see also Table S2).

(WISE) spectra (37), which correlate ^{13}C chemical shifts with ^{1}H−^{1}H dipole couplings (Figure 3b). These couplings, which are not completely suppressed under low MAS sample spinning (5 kHz), can be used to probe large-amplitude motions with rates larger than the dipole interaction.[37] Dipolar line shapes extracted from the Cα and Cβ region of both 2D-WISE spectra show a comparable line width, indicating similar dynamical properties of these D-residues independent of the state of bulk water.

In the liquid crystalline phase at 313 K, the intensities of ^{13}C-CP signals decrease notably as compared to at 273 K due to interference of intermediate time scale motions with ^{13}C-CP and ^{1}H decoupling (Figure 4a). To obtain more site-resolved details, we have recorded CC-DARR spectra in both lipid phases (Figure 4b). Although a good overlap is observed, at least 15 residues have been identified, which disappear from the liquid crystalline spectrum (see Table S2). They are found in the BC Loop (T86, E85, D88), along helix C (D97, V102, A114, A115, A116), in helix E (P150), in the EF loop (E170, P180), in helix F (S179, P201), and in helix G (V229, V241). Their locations in a homology model of PR are shown in Figure 5.

In contrast to CP, refocused ^{13}C-INEPT spectra of U-[^{13}C,^{15}N]$_{\backslash WHYFI}$-PR show a different temperature dependence. Peak intensities decrease 6−8 times in samples with frozen water (240 K) in the H(H)C-INEPT-HETCOR spectrum (Figure 6c) as compared to those with liquid water (273 K) (Figure 6a). This shows that liquid water is crucial for the high mobility of J-residues. The observation of some remaining J-residue signals at 240 K indicates the presence of nonfrozen hydration water. In the fluid phase, the intensities of ^{13}C-INEPT signals increase by 20−30% as compared to the gel phase. A comparison between HC-INEPT-HETCOR spectra recorded in both phases at 273

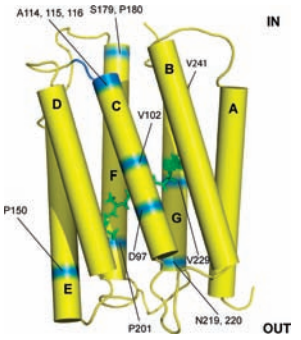

Figure 5. Modified homology model of green PR:[20] Helical residues influenced by changes in membrane elasticity (labeled in blue) are found in helices C, E, F, and G as well as in loops EC and EF. These residues disappear in the fluid membrane but are visible in the gel phase. This indicates that especially helices C and G but also E and F undergo thermal equilibrium fluctuations in the ground state of PR.

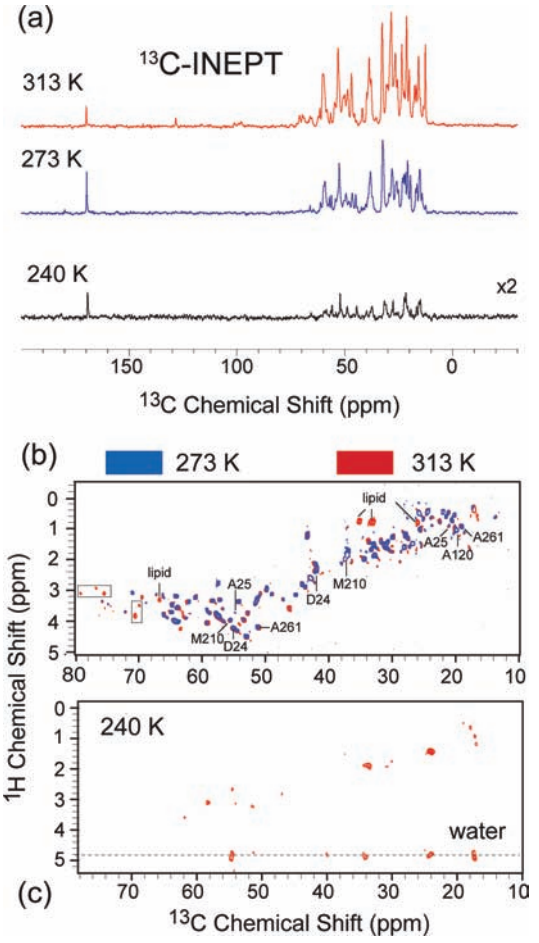

Figure 6. INEPT-based experiments of U-[^{13}C,^{15}N]$_{\backslash WHYFI}$-PR. (a) Refocused ^{13}C-INEPT spectra at three different temperatures. (b) Comparison of HC-INEPT-HETCOR spectra in lipid gel (blue) and liquid crystalline phase (red). (c) H(H)C-INEPT-HETCOR spectrum with 200 ms proton mixing acquired at 240 K with frozen bulk water. Water−protein cross peaks arise from water molecules within the first hydration layer on the protein surface.

and 313 K shows a very good overlap of all major resonances with an almost site-independent intensity enhancement in the fluid phase. This demonstrates that the increased mobility of

dx.doi.org/10.1021/ja109766n |J. Am. Chem. Soc. 2011, 133, 4874–4881

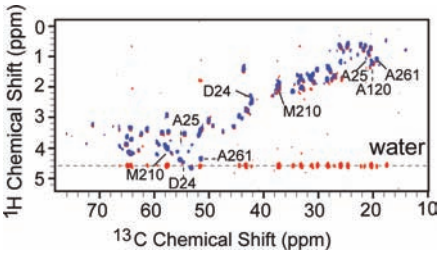

Figure 7. (a) Comparison of H(H)C-INEPT-HETCOR spectra of U-[^{13}C,^{15}N]$_{\backslash WHYFI}$-PR with (red) and without (blue) a 200 ms proton mixing step. Both spectra were acquired at 273 K. Water−protein correlations are seen along δ_{1H} = 4.7 ppm. The average peak intensities of residues with water contact in HC-INEPT HETCOR spectra are about 3 times higher than those without (see text and Tables S2 and S3).

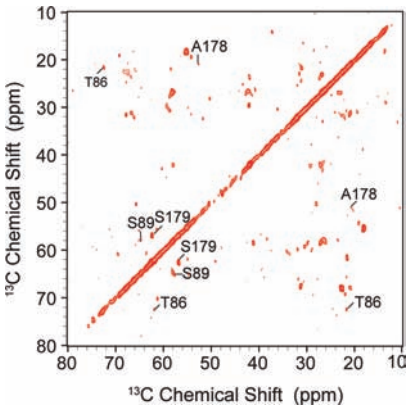

Figure 8. Water-edited CC-DARR spectrum of U-[^{13}C,^{15}N]-PR. This experiment shows amino acids in contact with mobile water. Four residues could be identified on the basis of their chemical shift. The spectrum was acquired at 273 K.

J-residues in the lipid fluid phase is more a direct consequence of a raise in temperature than a result of lipid phase transition.

c. Probing of Direct Water Interactions of J- and D-Residues. To probe to which extent J-residues are involved in direct water interaction, we have carried out H(H)C-INEPT-HETCOR experiments using a 200 ms longitudinal proton mixing step.[32] This mixing step allows magnetization transfer between water and protein protons and subsequently to ^{13}C nuclei in the protein via INEPT. A comparison between HC- and H(H)C-INEPT-HETCOR spectra is shown in Figure 7. Many additional cross peaks between ^{13}C protein backbone and side-chain resonances with water become visible when proton mixing is applied. A120 and M210 were identified to show a clear and unambiguous water contact. Interestingly, a strong correlation between peak intensities and water accessibilities of J-residues has been observed in HC-INEPT-HETCOR spectra. The average signal intensity of J-residues with water contact is about 3 times larger than those without (Tables S2 and S3). Higher peak intensities in these experiments are directly correlated with a longer effective proton spin−spin relaxation time ^{1}H-T$_2'$, hence higher mobility. This means that water facilitates fast, large amplitude motions for these residues.

The water accessibility of D-residues has also been probed by water-edited CC-DARR experiments (Figure 8). For that purpose, a 3 ms Gaussian soft pulse for selective water excitation followed by a 2 ms ^{1}H-T$_2'$ filter has been used.[38] This ensures

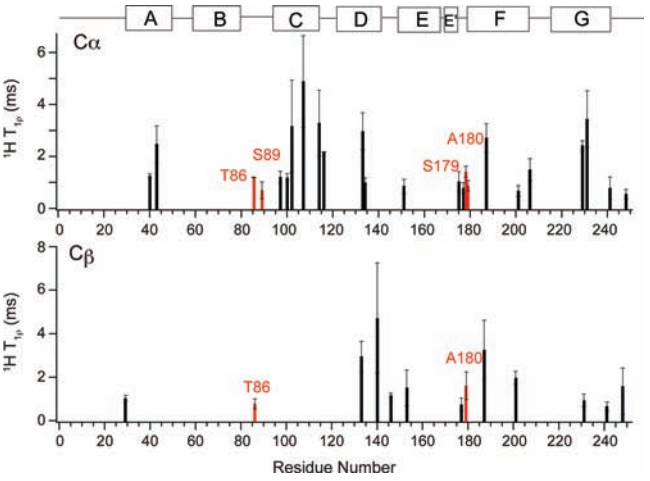

Figure 9. ^{1}H-T1ρ of Cα and Cβ plotted versus primary structure of U-[^{13}C,^{15}N]$_{\backslash WHYFI}$-PR. Secondary structure elements are indicated on top. The variation of T1ρ along the PR sequence is not very large, but residues in contact with water, or their next neighbors (red), do not show an enhanced mobility. See Figure S4 and Materials and Methods for further information.

that only ^{1}H magnetization from mobile water molecules is selected and transferred via a 4 ms spin diffusion step to protein protons. Detection takes place through ^{13}C-CP. As seen in Figure 8, many cross peaks are observed. Four residues (T86, S89, A178, S179) on the protein surface could be identified on the basis of their ^{13}C chemical shift assignment.

d. Probing Dynamics of D-Residues by ^{1}H-T1ρ Measurements. To characterize the molecular mobility of D-residues in PR in more detail, we measured ^{1}H spin−lattice relaxation times in the rotating frame (^{1}H-T1ρ), which are sensitive to motions at a time scale of 10^{-6} s. To ensure that these values only probe site-specific dynamics, we have used a very short ^{1}H−^{13}C cross-polarization contact time during which magnetization from directly bonded protons is transferred to carbons. The CP step itself takes place under Lee−Goldberg conditions, which ensures homonuclear proton decoupling and suppresses spin diffusion. Relaxation data from a number of isolated cross peaks were extracted from a series of CC-DARR spectra obtained from U-[^{13}C,^{15}N]$_{\backslash WHYFI}$-PR (Figure S4). Results are shown in Figure 9 for Cα and Cβ as a function of residue number. Overall, there is not a huge variation of relaxation times, which are found in the range of 1−6 ms. Residues located in transmembrane regions seem to have a higher average T1ρ as compared to those located on the protein surface. In Figure 9, the water-accessible residues identified in the spectrum of Figure 8 (or their next neighbors) are labeled in red. Their relaxation times do not differ from those of other residues in the same protein region for which no distinct water contact was found. Therefore, water does not seem to have a direct effect on the mobility of these residues.

DISCUSSION

a. PR Shows Heterogeneous Dynamics. In this study, we have characterized the molecular dynamics of PR in its ground state by solid-state NMR. We have identified 18 residues located in regions with fast, large amplitude motions (J-residues), while Shi et al.[15,16] have assigned 153 residues with restricted mobility (D-residues). The remaining residues are either not detectable or could not be assigned. The relatively small number of J-residues

dx.doi.org/10.1021/ja109766n |J. Am. Chem. Soc. 2011, 133, 4874–4881

and the large number of D-residues are within the expectations derived from the topology of this membrane protein (Figure 1c): Most residues are located within the transmembrane α-helical bundle, which imposes restrictions on motional amplitudes. Furthermore, residues in structured loops BC, DE (β-turn), and EF (α-helical) are also found within the "D-residue" category, although they show higher flexibility as compared to transmembrane segments as revealed by T1ρ experiments. In contrast to D-, all J-residues have been found in loop, tail, and the interface region of PR (labeled red in Figure 1c) on both the extracellular and the cytoplasmatic sides. Heterogeneous dynamics revealed by solid-state NMR has also been described for other α-helical membrane proteins such as BR, studied by ^{2}H NMR, or NpSRII investigated by MAS NMR.[10,39−42]

The surprisingly small contribution of N- and C-terminal residues (D24, A25, L260, A261)to the J-category can be explained by two reasons: (i) The N-terminal tail contains a hydrophobic signal peptide, which is partially cleaved off between residues 17 and 18 in *E. coli*,[14,18,21] and (ii) the mobility of the C-terminus seems to be restricted, as judged by the observation of His-tag signals in some CP experiments. The remaining of our assigned residues, V119, A120, are located in the CD-loop, and M210 is found in the FG-loop (see Figure 1c and Table S1). Comparing their ^{13}C chemical shifts (Cα/Cβ cross peak) with the ^{13}C chemical shift index, it is found that their values would be compatible with random coil (CG loop) or β-sheet (FG loop) structures.

b. The Dynamic of PR Is Affected by Water and Lipids in a Heterogeneous Way. *Water.* Every protein is surrounded by a hydration shell of about two layers of water and embedded in bulk solvent. Hydration shell and bulk solvent are essential for protein dynamics.[43] It has been suggested that water could act as a lubricant, which shields side-chain charges due to its high permittivity and is therefore smoothing side chain−side chain contacts.[44] Furthermore, the concept of "slaving" has been brought forward to discuss the control of protein dynamics by fluctuations in bulk water and hydration shell.[45] In case of membrane proteins, the models have to be extended toward a correlation between water dynamics and lipid and protein components.[46] Good progress has been made using mainly inelastic neutron scattering on bacteriorhodopsin in purple membrane[46] as well as magnetic relaxation dispersion methods.[47] Although a large range of time scales is accessible, the lack of a site resolution of this method only allows general statements about dynamic properties averaged over the whole protein or lipid structure. Such information can be provided by solid-state NMR as presented here. The exact mechanisms, which lead to magnetization exchange between water and protein protons, have been discussed in great detail for soluble proteins.[48,49] Mechanisms such as NOE, chemical exchange, and proton spin diffusion can all contribute making an exact differentiation between "bound" and free water difficult. Furthermore, it is important to realize that water molecules in the hydration layer are not bound in a thermodynamic or kinetic sense.[49] Water−protein transfer mechanisms in solid-state NMR have been investigated in detail for a microcrystalline protein.[50,51] Chemical exchange was found to provide a major pathway for magnetization transfer between protein surface and water. It has been shown for membrane proteins that a general interpretation of water correlation in terms of water accessibility, as found in the water-edited CC-DARR spectrum in Figure 8, is feasible in a site-specific manner.[38] For probing water contact of J-residues, we have used a longitudinal HH mixing step during which different protein−water magnetization exchange mechanisms could take place. It is currently not possible to differentiate between them, and we therefore restrict our data interpretation to the correlation between water accessibility and protein dynamics.

Our observations show that the mobility of J-residues is directly correlated with hydration, while D-residues are less influenced. This is concluded from our observation that J-residues in direct contact with hydration water show an increased peak intensity in HC-INEPT spectra caused by ^{1}H-T_2', which originates from higher mobility (Figure 7). Further support comes from freezing-induced dehydration of the protein−lipid complex, which leads to a dramatic suppression of most but not all resonances in the H(H)C-INEPT HETCOR experiment (Figure 6). With the freezing of bulk water, the thickness of the hydration layer significantly decreases, as shown by neutron diffraction studies on purple membrane.[4] This thinning of the hydration layer suppresses main and side-chain movement through a space reduction. The remaining cross peaks between water and protein observed in these frozen samples and the observation that a fluid hydration layer still exists at this temperature (Figure 2c) show that hydration water has a direct influence onto the dynamics of these residues. This is in line with other solid-state NMR studies, which did show that the first hydration layer is important for protein fluctuations.[52] This water hydration layers does not crystallize but shows a glass phase transition[53] and can therefore retain protein dynamics at lower temperatures. It has been also suggested to be involved in long-range lateral proton movement on the protein and membrane surface.[46] In contrast to J-residues, the effect of water onto the dynamics of D-residues is not as pronounced. Freezing-induced dehydration of PR did not change the intensity of CP spectra significantly, nor did it change ^{1}H lineshapes in 2D-WISE experiments, which report on motions in the submicrosecond time scale. In addition, D-residues for which a water interaction could be detected (Figure 8) do not show a higher mobility than residues without direct water contact in the same secondary structure element as revealed by T1ρ measurements (Figure 9). Reasons for the different hydration response of J- and D-residues could be either simply the limited water accessibility for segments located in the lipid bilayer resulting in stronger side-chain interactions and/or the steric restrictions due to the lipid environment, which have a stronger effect than water hydration.

The experiments presented here allow probing interaction with external hydration water. All identified residues with water contact are found on the protein surface. Other experimental approaches are needed to detect internal hydration within the protein or within the lipid bilayer. For example, a combination of selective labeling and H_2O/D_2O exchange with ^{15}N-CP has been used for BR[54] and PR[21] to detect internal water accessibility. The functional importance of internal water hydration has also been shown by solid-state NMR for the voltage-sensing domain[3] and for rhodopsin.[7]

Lipids. Alterations in membrane elasticity and bilayer thickness as induced by changing from the gel to the liquid crystalline phase had a clear location-dependent effect on some D- but not on J-residues: 15 residues could be identified, which disappear in the fluid phase (Figure 5, Table S2). This can be explained by thermal equilibrium fluctuations on the microsecond time scale, which would be blocked in the gel phase. Furthermore, the reduced bilayer thickness by 10−15% in the fluid phase could expose more residues to the solvent and hence display higher flexibility.

c. Functional Consequences from PR's Heterogeneous Dynamics. The identification of J-residues within PR (Figure 1c) did show that the cytoplasmatic BC-loop and the extracellular FG-loop undergo large amplitude fluctuations. Especially the mobility of the latter has been suggested to play an indirect role in proton release:[18] Unlike BR, PR does not have a proton release complex in the FG loop, but its flexibility could make buried residues involved in proton release (R94 or E142) accessible from the extracellular side. The location of the 15 D-residues affected by lipid main phase transition (Figure 5) allows one to identify protein regions that undergo thermal equilibrium fluctuations. Such fluctuations in ground-state PR have functional consequences, as this provides a stochastic mechanism to overcome energy barriers between different charge and conformational states during the photocycle. Especially helix C shows pronounced mobility, as five affected residues, including the primary proton acceptor D97, have been identified. In helix G, two residues have been found, one of those (V229) in close proximity to the Schiff base K231. This shows, together with the identification of N219 and N220 as J-residues, a high intrinsic mobility of helix G. Our data also show equilibrium fluctuations of the structured EF loop, for which an opening motion during the photocycle has been found to support proton uptake from the aqueous cytoplasmic side in BR.[55]

SUMMARY AND GENERAL CONCLUSION

The characterization of molecular dynamics of membrane proteins within lipid bilayers is of high relevance for understanding their functional mechanism at molecular level. Solid-state NMR is the only method that can provide site-resolved protein data within the lipid environment and is highly complementary with X-ray structure determination and neutron diffraction. We have been able to probe the influence of temperature, hydration, and membrane elasticity to PR segments with different secondary structure and dynamic. Our data show a clear correlation between hydration water and mobility of J-residues (mainly in flexible loops and tails), but only little effect was observed on D-residues (found in nonflexible loops and transmembrane domains). Changes in membrane elasticity did allow one to identify functional important regions with intrinsic equilibrium fluctuations. For a more detailed elucidation of PR's functional mechanism, further studies are needed at different states. In particular, the role of buried and surface associated water for proton pumping above and below the pK_a of D97 has been already the focus of our research and will be reported elsewhere.

MATERIALS AND METHODS

Expression, Purification, and Reconstitution of GPR. U-[^{13}C,^{15}N]-PR and reversely labeled in U-[^{13}C,^{15}N]$_{\backslash WHYFI}$-PR were expressed in *E. coli* and purified as described before.[22] The protein was reconstituted in DMPC:DMPA liposomes at a ratio of 9:1 (w/w). As compared to 2D crystalline preparations,[15,16] this lipid mixture allows highly homogeneous sample preparations as judged from the signal to noise ratio.[18] The pH was adjusted to 8.5 in 50 mM tricine. An amount of approximately 15 mg of protein was spun into a 4 mm MAS rotor. See the Supporting Information for further details.

NMR Experiments. All MAS NMR experiments were conducted using a 4 mm triple-resonance DVT HCN probe on a Bruker wide bore Avance III solid-state NMR spectrometer with ^{1}H frequency 850.32 MHz. 1D and 2D dipolar- and J-based experiments were conducted at 13 889 ± 2 Hz spinning rate with 70 kHz SPINAL64[56] ^{1}H-decoupling during ^{13}C chemical shift evolution and acquisition. A 3 s recycle delay time was used. A cross-polarization contact time of 0.7 ms was applied. ^{13}C-INEPT experiments were carried out using a refocused ^{1}H -^{13}C-INEPT step, with a 5 ms ^{1}H-T_2'-filter without ^{1}H−^{1}H decoupling during the refocusing delay. This ensures that only highly mobile ^{1}H spins with long T_2' were selected. ^{13}C−^{13}C through-space correlation spectroscopy was carried out using DARR[33] with a 50 ms mixing time after an initial CP step. ^{13}C−^{13}C through-bond spectra were recorded using TOBSY[31] with initial refocused INEPT step. The TOBSY experiment was acquired at 8 kHz sample spinning speed and with a 7.5 ms $P9^1_3$ mixing sequence and the ^{13}C-carrier frequency set to 100 ppm. H(H)C-INEPT-HETCOR experiments were essentially carried out as described in ref 32. A 200 ms HH-mixing time was used. Water-edited CC-DARR experiments[38] were conducted using a 3 ms Gaussian soft pulse for selective water excitation followed by a 2 ms ^{1}H-T_2' filter to select mobile water molecules only. Magnetization transfer to the protein took place via a 4 ms HH-mixing step prior to CP. ^{1}H-T1ρ measurements were done using CP under Lee−Goldberg conditions[57] with 300 μs contact time and 39 kHz ^{1}H-Lee−Goldberg offset to suppress ^{1}H−^{1}H spin diffusion (see the Supporting Information). An effective ^{1}H-spin lock field of 70 kHz of variable duration (0, 0.5, 1, 3, 5 ms) was applied to protons along the magic angle before the Lee−Goldberg-CP step. Site-specific values were obtained from a series of CC-DARR spectra acquired using different spin lock times (see Figure S4). WISE spectra[37] were recorded at 5 kHz spinning. In variable temperature experiments, the sample was equilibrated for 30 min at each temperature before probe tuning and spectra acquisition. The RF power level at different temperatures was calibrated, and CP and INEPT conditions were optimized before spectra recording. ^{13}C chemical shift referencing was carried out with respect to DSS through adamantane (40.49, 31.47 ppm).

ASSOCIATED CONTENT

Supporting Information. Further details regarding sample preparation, assignment of J-residues, ^{1}H-T1ρ experiments, and cross-peak intensities. This material is available free of charge via the Internet at http://pubs.acs.org.

AUTHOR INFORMATION

Corresponding Author
yangjun@wipm.ac.cn; glaubitz@em.uni-frankfurt.de

ACKNOWLEDGMENT

This work was funded by the EU FP6 "PRISM" project and the DFG through SFB 807 "Membrane Transport". Additional support by the Frankfurt Cluster of Excellence "Macromolecular Complexes" is acknowledged. J.Y. was the recipient of a Humboldt Foundation fellowship and acknowledges support by the National Natural Science Foundation of China (20921004) and the National Basic Research Program of China (2009CB918600). DFG is acknowledged for an equipment grant (GL 307/2-1).

REFERENCES

(1) Wood, K.; Plazanet, M.; Gabel, F.; Kessler, B.; Oesterhel, D.; Tobias, D. J.; Zaccai, G.; Weik, M. *Proc. Natl. Acad. Sci. U.S.A.* **2007**, *104*, 18049–18054.
(2) Lee, A. G. *Biochim. Biophys. Acta, Biomembr.* **2003**, *1612*, 1–40.
(3) Krepkiy, D.; Mihailescu, M.; Freites, J. A.; Schow, E. V.; Worcester, D. L.; Gawrisch, K.; Tobias, D. J.; White, S. H.; Swartz, K. J. *Nature* **2009**, *462*, 473–U168.
(4) Fitter, J.; Lechner, R. E.; Dencher, N. A. *J. Phys. Chem. B* **1999**, *103*, 8036–8050.

(5) Fitter, J.; Verclas, S. A. W.; Lechner, R. E.; Seelert, H.; Dencher, N. A. *FEBS Lett.* **1998**, *433*, 321–325.
(6) Sharpe, S.; Yau, W. M.; Tycko, R. *Biochemistry* **2006**, *45*, 918–933.
(7) Grossfield, A.; Pitman, M. C.; Feller, S. E.; Soubias, O.; Gawrisch, K. *J. Mol. Biol.* **2008**, *381*, 478–486.
(8) Patargias, G.; Bond, P. J.; Deol, S. S.; Sansom, M. S. P. *J. Phys. Chem. B* **2005**, *109*, 575–582.
(9) Jang, H.; Crozier, P. S.; Stevens, M. J.; Woolf, T. B. *Biophys. J.* **2004**, *87*, 129–145.
(10) Etzkorn, M.; Martell, S.; Andronesi, O. C.; Seidel, K.; Engelhard, M.; Baldus, M. *Angew. Chem., Int. Ed.* **2007**, *46*, 459–462.
(11) Beja, O.; Aravind, L.; Koonin, E. V.; Suzuki, M. T.; Hadd, A.; Nguyen, L. P.; Jovanovich, S. B.; Gates, C. M.; Feldman, R. A.; Spudich, J. L.; Spudich, E. N.; DeLong, E. F. *Science* **2000**, *289*, 1902–6.
(12) Sabehi, G.; Loy, A.; Jung, K. H.; Partha, R.; Spudich, J. L.; Isaacson, T.; Hirschberg, J.; Wagner, M.; Beja, O. *PLoS Biol.* **2005**, *3*, e273.
(13) Walter, J. M.; Greenfield, D.; Bustamante, C.; Liphardt, J. *Proc. Natl. Acad. Sci. U.S.A.* **2007**, *104*, 2408–12.
(14) Friedrich, T.; Geibel, S.; Kalmbach, R.; Chizhov, I.; Ataka, K.; Heberle, J.; Engelhard, M.; Bamberg, E. *J. Mol. Biol.* **2002**, *321*, 821–38.
(15) Shastri, S.; Vonck, J.; Pfleger, N.; Haase, W.; Kuehlbrandt, W.; Glaubitz, C. *Biochim. Biophys. Acta, Biomembr.* **2007**, *1768*, 3012–3019.
(16) Klyszejko, A. L.; Shastri, S.; Mari, S. A.; Grubmuller, H.; Muller, D. J.; Glaubitz, C. *J. Mol. Biol.* **2008**, *376*, 35–41.
(17) Hoffman, J.; Aslimovska, L.; Bamann, C.; Glaubitz, C.; Bamberg, E.; Brutschy, B. *Phys. Chem. Chem. Phys.* **2010**, *12*, 3480–3485.
(18) Shi, L. C.; Ahmed, M. A.; Zhang, W.; Whited, G.; Brown, L. S.; Ladizhansky, V. *J. Mol. Biol.* **2009**, *386*, 1078–93.
(19) Shi, L. C.; Lake, E. M. R.; Ahmed, M. A. M.; Brown, L. S.; Ladizhansky, V. *Biochim. Biophys. Acta, Biomembr.* **2009**, *1788*, 2563–2574.
(20) Rangarajan, R.; Galan, J. F.; Whited, G.; Birge, R. R. *Biochemistry* **2007**, *46*, 12679–86.
(21) Pfleger, N.; Worner, A. C.; Yang, J.; Shastri, S.; Hellmich, U. A.; Aslimovska, L.; Maier, M. S. M.; Glaubitz, C. *Biochim. Biophys. Acta, Bioenerg.* **2009**, *1787*, 697–705.
(22) Pfleger, N.; Lorch, M.; Woerner, A. C.; Shastri, S.; Glaubitz, C. *J. Biomol. NMR* **2008**, *40*, 15–21.
(23) Andersson, M.; Malmerberg, E.; Westenhoff, S.; Katona, G.; Cammarata, M.; Wohri, A. B.; Johansson, L. C.; Ewald, F.; Eklund, M.; Wulff, M.; Davidsson, J.; Neutze, R. *Structure* **2009**, *17*, 1265–75.
(24) Hong, M. *J. Phys. Chem. B* **2007**, *111*, 10340–10351.
(25) McDermott, A. *Annu. Rev. Biophys.* **2009**, *38*, 385–403.
(26) Huster, D. *Prog. Nucl. Magn. Reson. Spectrosc.* **2005**, *46*, 79–107.
(27) Durr, U. H. N.; Yamamoto, K.; Im, S. C.; Waskell, L.; Ramamoorthy, A. *J. Am. Chem. Soc.* **2007**, *129*, 6670–6671.
(28) Yang, J.; Tasayco, M. L.; Polenova, T. *J. Am. Chem. Soc.* **2009**, *131*, 13690–13702.
(29) Lorieau, J. L.; McDermott, A. E. *J. Am. Chem. Soc.* **2006**, *128*, 11505–11512.
(30) Chevelkov, V.; Fink, U.; Reif, B. *J. Am. Chem. Soc.* **2009**, *131*, 14018–14022.
(31) Baldus, M.; Meier, B. H. *J. Magn. Reson., Ser. A* **1996**, *121*, 65–69.
(32) Andronesi, O. C.; Becker, S.; Seidel, K.; Heise, H.; Young, H. S.; Baldus, M. *J. Am. Chem. Soc.* **2005**, *127*, 12965–12974.
(33) Takegoshi, K.; Nakamura, S.; Terao, T. *Chem. Phys. Lett.* **2001**, *344*, 631–637.
(34) Wishart, D. S.; Sykes, B. D. *J. Biomol. NMR* **1994**, *4*, 171–180.
(35) Su, Y. C.; Mani, R.; Doherty, T.; Waring, A. J.; Hong, M. *J. Mol. Biol.* **2008**, *381*, 1133–1144.
(36) Tuzi, S.; Naito, A.; Saito, H. *Eur. J. Biochem.* **1996**, *239*, 294–301.
(37) Schmidt-Rohr, K.; Clauss, J.; Spiess, H. W. *Macromolecules* **1992**, *25*, 3273–3277.
(38) Ader, C.; Schneider, R.; Seidel, K.; Etzkorn, M.; Becker, S.; Baldus, M. *J. Am. Chem. Soc.* **2009**, *131*, 170–176.
(39) Siarheyeva, A.; Lopez, J. J.; Lehner, I.; Hellmich, U. A.; van Veen, H. W.; Glaubitz, C. *Biochemistry* **2007**, *46*, 3075–3083.
(40) Smith, R. L.; Oldfield, E. *Science* **1984**, *225*, 280–288.
(41) Leo, G. C.; Colnago, L. A.; Valentine, K. G.; Opella, S. J. *Biochemistry* **1987**, *26*, 854–862.
(42) Keniry, M. A.; Gutowsky, H. S.; Oldfield, E. *Nature* **1984**, *307*, 383–386.
(43) Frauenfelder, H.; Chen, G.; Berendzen, J.; Fenimore, P. W.; Jansson, H.; McMahon, B. H.; Stroe, I. R.; Swenson, J.; Young, R. D. *Proc. Natl. Acad. Sci. U.S.A.* **2009**, *106*, 5129–5134.
(44) Cinelli, S.; De Francesco, A.; Onori, G.; Paciaroni, A. *Phys. Chem. Chem. Phys.* **2004**, *6*, 3591–3595.
(45) Fenimore, P. W.; Frauenfelder, H.; McMahon, B. H.; Parak, F. G. *Proc. Natl. Acad. Sci. U.S.A.* **2002**, *99*, 16047–16051.
(46) Dencher, N. A.; Sass, H. J.; Buldt, G. *Biochim. Biophys. Acta* **2000**, *1460*, 192–203.
(47) Gottschalk, M.; Dencher, N. A.; Halle, B. *J. Mol. Biol.* **2001**, *311*, 605–621.
(48) Otting, G. *Prog. Nucl. Magn. Reson. Spectrosc.* **1997**, *31*, 259–285.
(49) Halle, B. *Philos. Trans. R. Soc. London, Ser. B* **2004**, *359*, 1207–1223.
(50) Lesage, A.; Gardiennet, C.; Loquet, A.; Verel, R.; Pintacuda, G.; Emsley, L.; Meier, B. H.; Bockmann, A. *Angew. Chem., Int. Ed.* **2008**, *47*, 5851–5854.
(51) Lesage, A.; Bockmann, A. *J. Am. Chem. Soc.* **2003**, *125*, 13336–13337.
(52) Reichert, D.; Pascui, O.; deAzevedo, E. R.; Bonagamba, T. J.; Arnold, K.; Huster, D. *Magn. Reson. Chem.* **2004**, *42*, 276–284.
(53) Tarek, M.; Tobias, D. J. *Biophys. J.* **2000**, *79*, 3244–3257.
(54) Mason, A. J.; Turner, G. J.; Glaubitz, C. *FEBS J.* **2005**, *272*, 2152–2164.
(55) Lanyi, J. K.; Luecke, H. *Curr. Opin. Struct. Biol.* **2001**, *11*, 415–419.
(56) Fung, B. M.; Khitrin, A. K.; Ermolaev, K. *J. Magn. Reson.* **2000**, *142*, 97–101.
(57) Lee, M.; Goldburg, W. I. *Phys. Rev.* **1965**, *140*, 1261–1271.